PKR and RNase L Contribute to Protection against Lethal West Nile Virus Infection by Controlling Early Viral Spread in the Periphery and Replication in Neurons

Melanie A. Samuel,[1] Kevin Whitby,[2]† Brian C. Keller,[3] Anantha Marri,[2] Winfried Barchet,[4] Bryan R. G. Williams,[5]‡ Robert H. Silverman,[5] Michael Gale, Jr.,[3] and Michael S. Diamond[1,2,4]*

Departments of Molecular Microbiology,[1] Medicine,[2] and Pathology & Immunology,[4] Washington University School of Medicine, St. Louis, Missouri 63110; Department of Microbiology, University of Texas Southwestern Medical Center, Dallas, Texas 75390-9048[3]; and Department of Cancer Biology/NB40, Lerner Research Institute, The Cleveland Clinic Foundation, Cleveland, Ohio 44195[5]

West Nile virus (WNV) is a neurotropic, mosquito-borne flavivirus that can cause lethal meningoencephalitis. Type I interferon (IFN) plays a critical role in controlling WNV replication, spread, and tropism. In this study, we begin to examine the effector mechanisms by which type I IFN inhibits WNV infection. Mice lacking both the interferon-induced, double-stranded-RNA-activated protein kinase (PKR) and the endoribonuclease of the 2′,5′-oligoadenylate synthetase-RNase L system (PKR$^{-/-}$ × RL$^{-/-}$) were highly susceptible to subcutaneous WNV infection, with a 90% mortality rate compared to the 30% mortality rate observed in congenic wild-type mice. PKR$^{-/-}$ × RL$^{-/-}$ mice had increased viral loads in their draining lymph nodes, sera, and spleens, which led to early viral entry into the central nervous system (CNS) and higher viral burden in neuronal tissues. Although mice lacking RNase L showed a higher CNS viral burden and an increased mortality, they were less susceptible than the PKR$^{-/-}$ × RL$^{-/-}$ mice; thus, we also infer an antiviral role for PKR in the control of WNV infection. Notably, a deficiency in both PKR and RNase L resulted in a decreased ability of type I IFN to inhibit WNV in primary macrophages and cortical neurons. In contrast, the peripheral neurons of the superior cervical ganglia of PKR$^{-/-}$ × RL$^{-/-}$ mice showed no deficiency in the IFN-mediated inhibition of WNV. Our data suggest that PKR and RNase L contribute to IFN-mediated protection in a cell-restricted manner and control WNV infection in peripheral tissues and some neuronal subtypes.

West Nile virus (WNV) is a neurotropic flavivirus that, in nature, cycles through mosquitoes and birds and can infect humans and other mammals. Humans develop a febrile illness that can progress to neurological disease, including encephalitis, meningitis, and poliomyelitis (3, 8, 43, 44, 65). Initial viral replication is thought to occur in skin Langerhans' dendritic cells, followed by seeding of draining lymph nodes and viremia (6, 33). WNV crosses into the central nervous system (CNS) through an undefined mechanism that may involve tumor necrosis factor-α-mediated changes in blood-brain barrier permeability (73). Upon CNS entry, WNV infects and injures several different neuronal cell populations, including those in the cerebral cortex, brain stem, hippocampus, and spinal cord (14, 19, 21, 55, 68, 76).

In humans, increased disease susceptibility is correlated with depressed immunity and increased age (11, 29, 32, 39). The immunologic basis for resistance to flaviviruses has begun to be elucidated using rodent models and human genetic analysis. Humoral immunity and cytotoxic-T-lymphocyte responses are important in controlling WNV infection and spread, as both

B-cell- and CD8$^+$ T-cell-deficient mice showed significantly increased viral burden and lethality (14, 68a, 73a). In humans, a defective allele for the chemokine receptor CCR5 has been linked to an increased risk for symptomatic WNV infection (26); in mice, a deficiency in CCR5 is associated with decreased leukocyte trafficking to the CNS and a higher viral burden (25). Less is known regarding the mechanisms by which innate immunity controls flavivirus infection. Recent studies suggest that host cells respond to WNV through retinoic acid-inducible gene I (RIG-I)- and interferon regulatory factor 3 (IRF-3)-dependent pathways, resulting in the production of several interferon (IFN)-stimulated genes and the inhibition of cell-to-cell spread (22, 23). Several flavivirus nonstructural proteins antagonize this antiviral response by impairing IFN gene transcription and type I IFN signaling (30, 46–48, 54). Although flaviviruses can counter IFN-induced responses within infected cells, IFN is still essential for limiting viral dissemination in vivo (49, 62, 67). After WNV infection, type I IFN is produced in both the serum and the brain, and a deficiency in the IFN-α/β receptor (IFN-α/βR$^{-/-}$) in mice resulted in uncontrolled viral replication, swift spread to the CNS, altered viral tropism, and rapid lethality (62). Although type I IFN is critical for the defense against flavivirus infections, the specific downstream antiviral effector mechanisms remain largely uncharacterized.

Type I IFNs induce an antiviral state within cells through the upregulation and activation of an array of antiviral effector molecules (reviewed in reference 57). Among these, the double-stranded RNA (dsRNA)-dependent protein kinase (PKR)

* Corresponding author. Mailing address: Department of Medicine, Molecular Microbiology, Pathology & Immunology, Washington University School of Medicine, Campus Box 8051, 660 S. Euclid Ave., St. Louis, MO 63110. Phone: (314) 362-2842. Fax: (314) 362-9230. E-mail address: diamond@borcim.wustl.edu.

† Present address: Discovery Biology, Pfizer Global Research and Development, Sandwich Laboratories, Sandwich, Kent CT13 9NJ, United Kingdom.

‡ Present address: Monash Institute of Medical Research, Monash University, 27-31 Wright Street, Clayton, Victoria 3168, Australia

and 2′,5′-oligoadenylate synthetase (OAS) proteins act as key mediators of intracellular resistance to several viruses (70, 75). PKR undergoes autophosphorylation after binding dsRNA and/or the PKR-activating (PACT) protein. The α subunit of eukaryotic translation initiation factor 2 (eIF2-α) is a central target for phosphorylation by activated PKR, resulting in a block of protein synthesis (52). OAS enzymes are activated by dsRNA to synthesize 2′,5′-linked oligoadenylates (36), which then bind and activate RNase L, an endoribonuclease that cleaves viral RNA and mRNA, leading to a decrease in protein synthesis and viral replication (69). In vitro, disparate cell populations have shown distinct dependencies on PKR and RNase L to modulate the replication of different viruses. Increased basal replication and persistence by the alphavirus Sindbis were observed in RNase L-deficient mouse embryonic fibroblasts (MEFs) and in bone marrow-derived dendritic cells (BM-DCs) of $PKR^{-/-} \times RL^{-/-}$ mice (60, 63). Despite this increased viral production, the IFN responsiveness of these cells remained largely intact in the absence of PKR and RNase L (59, 60). In contrast, PKR-deficient MEFs showed decreased type I IFN-mediated protection from vesicular stomatitis virus (VSV) infection (71), and PKR partially mediated the antiviral effects of IFN-β against herpes simplex virus (HSV) in trigeminal ganglion neurons (2). Members of the *Flaviviridae* family of RNA viruses also have exhibited varied sensitivities to PKR and RNase L in vitro. Although RNase L-deficient MEFs supported increased WNV replication, this phenotype appeared independent of IFN (64). Consistent with this, the absence of PKR and RNase L did not alter the IFN-β-mediated inhibition of dengue virus (13). In contrast, both effector molecules were implicated in the control of hepatitis C virus polyprotein production (27).

Despite the accumulation of in vitro data, the roles of PKR and RNase L have not been directly tested in vivo for any *Flaviviridae* family member. These proteins do, however, partially mediate antiviral resistance in mice for some viruses. Mice lacking PKR showed increased lethality following VSV infection (16, 71) and more severe ocular HSV disease (7). Mice deficient in PKR and/or RNase L showed increased mortality following coxsackievirus infection (20). In contrast, $PKR^{-/-} \times RL^{-/-}$ mice showed no increase in morbidity or mortality following alphavirus Sindbis virus infection, although increased viral loads in draining lymph nodes were observed (60). Thus, the ability of PKR and RNase L to mediate IFN-induced protection appears to vary across families of DNA and RNA viruses. Herein, we directly evaluate the roles of PKR and RNase L in controlling WNV replication and dissemination in mice and compare these to their antiviral effects in primary cells.

MATERIALS AND METHODS

Viruses. The WNV strain (3000.0259) was isolated in New York in 2000 after the inoculation of a mosquito homogenate onto Vero cells as previously described (18) and passaged once in C6/36 cells to generate a stock virus that was used in all experiments.

Mouse experiments and quantitation of viral burden. C57BL/6 wild-type inbred mice were obtained commercially (Jackson Laboratories, Bar Harbor, ME). $RL^{-/-}$ (81) and $PKR^{-/-} \times RL^{-/-}$ mice (78, 82) that were backcrossed 10 generations into the C57BL/6 background were genotyped and bred in the animal facility of Washington University School of Medicine, and experiments were performed in accordance with Washington University's animal studies guidelines. Eight- to ten-week-old mice were used for all in vivo studies. Peripheral infection was performed by footpad inoculation of 10^2 PFU of virus diluted in Hanks balanced salt solution (HBSS) with 1% heat-inactivated fetal bovine serum (FBS). Intracranial (IC) inoculation was performed using a tuberculin syringe with 10^1 PFU of virus diluted in 10 μl HBSS with 1% FBS. To examine the kinetics of viral spread and replication, mice were infected with 10^2 PFU of virus by footpad inoculation and euthanized on days 1, 2, 3, 4, 6, 8, and 10 after infection. Blood was collected by phlebotomy from the axillary vein, and sera were recovered, aliquoted, and stored at −80°C. To determine viral titers, mice were perfused with 10 to 20 ml of phosphate-buffered saline and organs were removed, weighed, and homogenized. Plaque assays were performed as previously described using BHK21 cells (14). Viral RNA was prepared from aliquots of sera with a Qia-Amp RNA recovery kit and from inguinal lymph nodes with an RNEasy kit according to the manufacturer's instructions (QIAGEN, Valencia, CA). WNV RNA was quantitated by real-time fluorogenic reverse transcription (RT)-PCR as described previously (14) using the following primers and probe to the *E* gene of WNV: the forward primer 5′-TCAGCGATCTCTCCA CCAAAG-3′, the reverse primer 5′-GGGTCAGCACGTTTGTCATTG-3′, and the probe 5′-FAM (6-carboxyfluorescein)-TGCCCGACCATGGGAGAAGCT C-3′-TAMRA (6-carboxytetramethylrhodamine) (42). To normalize lymph node RNA samples, fluorogenic RT-PCR was performed in parallel on 18S rRNA (Applied Biosystems, Foster City, CA).

IFN levels in serum. The level of biologically active type I IFN in serum was determined using an encephalomyocarditis virus (EMCV) bioassay of L929 cells as previously described (4). Briefly, 8- to 9-week-old C57BL/6 and congenic $PKR^{-/-} \times RL^{-/-}$ mice were infected by footpad inoculation with 10^2 PFU, and serum samples were harvested on days 1, 2, 3, 4, and 5 after infection, as described above. Serial dilutions of sera in Dulbecco's modified Eagle's medium (DMEM) containing 10% FBS were applied in duplicate to monolayers of L929 cells (1.8×10^4 cells/well) in 96-well plates. Following incubation for 14 h at 37°C, cells were infected with EMCV diluted in DMEM containing 2% FBS at a multiplicity of infection (MOI) of 7. Cells were inspected for cytopathic effect, and 7 hours postinfection, IFN-mediated protection was assayed using a CellTiter 96 aqueous cell proliferation assay as per the manufacturer's instructions (Promega Corporation, Madison, WI).

Strand-specific real-time RT-PCR. Strand-specific real-time RT-PCR was performed as previously described (62). Briefly, spleens were dissected from WNV-infected wild-type C57BL/6 and congenic $RL^{-/-}$ and $PKR^{-/-} \times RL^{-/-}$ mice on day 4, and single-cell suspensions were generated following treatment with type IV collagenase for 30 min at 37°C (Worthington Biochemical, Lakewood, NJ). Cells were washed with DMEM, and CD11b$^+$, CD11c$^+$, and CD19$^+$ cells were isolated by positive selection using antibody-conjugated magnetic beads as per the manufacturer's instructions (Miltenyi Biotec, Auburn, CA). Cell purity was assessed by flow cytometry using fluorescent conjugated antibodies against CD11b, CD11c, and B220 antigens (BD Pharmingen, San Diego, CA). RNA was extracted from purified cells using an RNEasy kit as per the manufacturer's instructions (QIAGEN). Strand-specific reverse transcription was performed for 30 min at 55°C using T7-tagged primers as previously described (62). Following a 10-min incubation at 95°C to inactivate the reverse transcriptase, 5 pmol of the probe (5′-FAM-CAACCTCACCTACAGGGCGGACTTCAAG-TAMRA-3′) and 20 pmol each of primers T7 and E1160F were added to positive-strand reaction mixtures and primers T7 and E1229R were added to negative-strand reaction mixtures. The thermal cycling reaction was then allowed to proceed (40 cycles of 95°C for 15 s and then 60°C for 1 min). To normalize the samples, the amount of 18S rRNA (Applied Biosystems) in each sample was determined by fluorogenic RT-PCR, performed in parallel assays.

Primary-cell cultures. Bone marrow-derived macrophages (BM-Mϕ) and dendritic cells (BM-DCs) were generated as described previously (9, 72) with the following modifications. Briefly, bone marrow cells derived from C57BL/6 wild-type and congenic $PKR^{-/-} \times RL^{-/-}$ and $RL^{-/-}$ mice were cultured in 12-well plates at a density of 1.5×10^5 cells per well. BM-Mϕ were grown in DMEM supplemented with 10% defined fetal calf serum (HyClone), 40 ng/ml macrophage colony-stimulating factor (M-CSF) (PeproTech, Inc., Rocky Hill, NJ), sodium pyruvate, penicillin-streptomycin, and glutamine for 6 days. BM-DCs were cultured in RPMI medium supplemented with 10% defined fetal calf serum (HyClone), 20 ng/ml granulocyte-macrophage colony-stimulating factor, 20 ng/ml interleukin 4 (PeproTech, Inc., Rocky Hill, NJ), sodium pyruvate, kanamycin sulfate, nonessential amino acids, and glutamine for 6 days. Beginning on day 7, BM-Mϕ and BM-DCs were maintained in 20 ng/ml M-CSF or 10 ng/ml granulocyte-M-CSF and 10 ng/ml interleukin 4, respectively. All bone marrow-derived cell experiments were performed on cells cultured for 7 to 8 days. Purity was determined by flow cytometry following staining with an anti-F4/80 antibody (BM-Mϕ) (Serotec, Inc., Raleigh, NC) or an anti-CD11c$^+$ antibody (BM-DCs)

(BD Pharmingen, San Diego, CA). Primary cortical neurons were prepared from day 15 C57BL/6 and congenic RL$^{-/-}$ and PKR$^{-/-} \times$ RL$^{-/-}$ mouse embryos essentially as previously described (38, 80). Cortical neuron experiments were performed using neurons that were cultured for 3 to 4 days. Primary sympathetic neuronal cultures were generated from superior cervical ganglia (SCG) of 1-day-old mice as reported previously (17). The purity of SCG cultures was determined via staining with anti-NeuN and anti-GFAP antibodies ($\sim$98 to 99%) (58). All SCG neuron experiments were performed on neurons cultured 6 to 7 days prior to treatment or infection.

IFN treatment of primary cells and virus infection. To assay IFN inhibition of WNV replication, BM-Mϕ, BM-DCs, and cortical and SCG neurons were treated with 100 IU/ml (neurons) or 1,000 IU/ml (bone marrow-derived cells) of mouse IFN-α, IFN-β, or IFN-γ (PBL Laboratories, Madison, WI) 24 h prior to infection or at the time of infection. Cortical neurons were infected at an MOI of 0.1 and SCG neurons at an MOI of 10 for 1 h, followed by extensive washing to remove free virus. Supernatants were harvested at 24 h postinfection. To determine WNV growth kinetics in BM-Mϕ and BM-DCs, cells were infected at an MOI of 0.01 for 1 h and washed extensively, and supernatants were harvested at 6, 24, and 48 h postinfection. The production of infectious virus was measured by a plaque assay on Vero cells as described previously (14).

Western blotting. Cortical neurons were lysed in radioimmunoprecipitation assay buffer (10 mM Tris, 150 mM NaCl, 0.02% sodium azide, 1% sodium deoxycholate, 1% Triton X-100, 0.1% sodium dodecyl sulfate, pH 7.4) with protease inhibitors (Sigma). Samples (30 μg) were resolved on 10% sodium dodecyl sulfate-polyacrylamide gels. Following transfer, membranes were blocked with 5% nonfat dried milk overnight at 4°C. Membranes were probed with the following panel of monoclonal or polyclonal antibodies: phosphorylated anti-PKR and anti-eIF2α (Cell Signaling), anti-eIF2α (24), anti-PKR and anti-GAPDH (glyceraldehyde-3-phosphate dehydrogenase) (Santa Cruz Biotechnology), anti-mouse IRF-3 (Zymed Laboratories), anti-mouse interferon-stimulated gene 56 (ISG56) and anti-mouse ISG54 (kind gifts from Ganes Sen), and anti-WNV (Centers for Disease Control and Prevention). Blots were subsequently incubated with peroxidase-conjugated secondary antibodies (Jackson Immunoresearch) and visualized using ECL-Plus immunoblotting reagents (Amersham Biosciences).

Statistical analysis. For in vitro experiments, an unpaired t test was used to determine significant differences. For viral burden analysis, differences in log titers were analyzed by the Mann-Whitney test. Kaplan-Meier survival curves were analyzed by the log rank test. All data were analyzed using Prism software (GraphPad, San Diego, CA).

RESULTS

Effect of RNase L and PKR on WNV pathogenesis in mice. Mice lacking the type I IFN receptor show extreme susceptibility to peripheral WNV infection, with 100% mortality by day 5 postinfection (62). Type I IFN restricts intracellular viral replication by inducing and activating an array of antiviral effector molecules. To investigate the mechanisms by which type I IFN controls WNV infection, we evaluated survival rates of mice lacking two key IFN-induced effector proteins, PKR and RNase L. After their footpads were inoculated with 10^2 PFU of WNV, mice lacking both PKR and RNase L (PKR$^{-/-} \times$ RL$^{-/-}$) showed acute clinical symptoms by day 8 to 9 postinfection, including a hunchback posture, weight loss, fur ruffling, and reduced activity. Although wild-type mice that progressed to death showed similar clinical signs, the rate and severity of clinical manifestations were lower. PKR$^{-/-} \times$ RL$^{-/-}$ mice were more vulnerable to lethal WNV infection, with a 10% survival rate compared to 70% for wild-type mice ($P < 0.0001$) (Fig. 1A). RNase L-deficient mice (RL$^{-/-}$) also showed an increased susceptibility to WNV infection (51% survival; $P = 0.03$), although they were less vulnerable than mice lacking both PKR and RNase L. These results suggest that the activities of PKR and RNase L play nonredundant, important roles in protecting mice from fatal WNV infection.
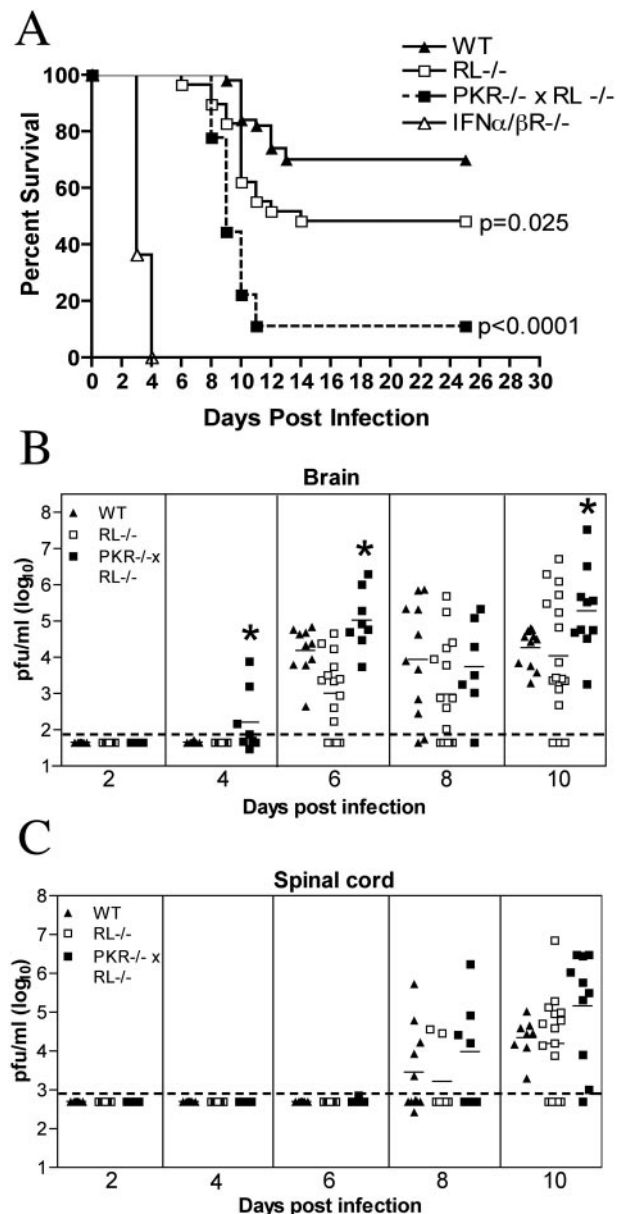

FIG. 1. Survival and virologic analysis for wild-type (WT), RL$^{-/-}$, PKR$^{-/-} \times$ RL$^{-/-}$, and IFN-α/βR$^{-/-}$ C57BL/6 mice. (A) Eight- to 10-week-old mice were inoculated with 10^2 PFU of WNV by footpad injection and followed for mortality for 25 days. The number of mice in these experiments was as follows: 50 wild-type, 29 RL$^{-/-}$, 18 PKR$^{-/-} \times$ RL$^{-/-}$, and 11 IFN-α/βR$^{-/-}$ mice. Survival differences between wild-type and all immunodeficient mice were statistically significant ($P \leq 0.03$). (B and C) Viral burdens in the CNS after WNV infection. Viral loads in the brain (B) and spinal cord (C) were determined from samples harvested on days 2, 4, 6, 8, and 10 using a viral plaque assay on BHK21 cells. Data are shown as the PFU per gram of tissue for 5 to 17 mice per time point. For all viral load data, the solid line represents the mean PFU per gram at the indicated time point, and the dotted line represents the limit of sensitivity of the assay. Asterisks indicate values that are statistically significant ($P < 0.05$) compared to those for wild-type mice.

PKR and RNase L are required for controlling WNV infection in mice. Because PKR and RNase L function to restrict intracellular viral replication (5, 28, 37, 45), we predicted that the enhanced lethality of mice lacking these effectors would

correlate with increased viral burdens. To evaluate this, $RL^{-/-}$, $PKR^{-/-} \times RL^{-/-}$, and wild-type mice were infected with 10^2 PFU, and CNS tissues were harvested on days 2, 4, 6, 8, and 10 after infection. Though dissemination rates and viral loads in the brains of $RL^{-/-}$ mice were largely indistinguishable from those in wild-type mice, mice that lacked both PKR and RNase L showed earlier WNV entry into the CNS and enhanced infection (Fig. 1B). At day 4, infectious WNV was present in the brains of 50% (four of eight) of the $PKR^{-/-} \times RL^{-/-}$ mice compared to 0% (zero of eight) of the wild-type mice. $PKR^{-/-} \times RL^{-/-}$ mice continued to show significantly increased viral burdens in their brains on day 6 after infection ($10^{5.0}$ PFU/g versus $10^{3.9}$ PFU/g; $P < 0.05$). By day 10, $PKR^{-/-} \times RL^{-/-}$ mice averaged 10-fold-higher viral titers than wild-type mice, corresponding with increased symptoms and death ($P = 0.03$). In contrast, the kinetics and magnitude of the viral burdens in the spinal cords of $RL^{-/-}$ and $PKR^{-/-} \times RL^{-/-}$ mice were not statistically different from those of the wild-type mice, although viral burdens in the $PKR^{-/-} \times RL^{-/-}$ mice trended toward higher levels after day 8 (Fig. 1C).

PKR and RNase L control early viral replication in peripheral lymphoid tissues. WNV is believed to replicate in skin dendritic cells, resulting in seeding of the draining lymph node and viremia (6, 33). Type I IFN is essential for limiting WNV replication soon after infection, as mice lacking the IFN-α/β receptor demonstrated high levels of infectious virus in their sera and spleens at early time points (62). Because we observed early WNV entry into the brains of $PKR^{-/-} \times RL^{-/-}$ mice, we speculated that PKR and RNase L modulated WNV replication in peripheral tissues. To examine this, viral levels in the lymph node, spleen, and serum were determined during early stages of infection.

(i) Lymph node. Viral RNA levels were assayed in the draining lymph node that was ipsilateral to the infection site by a quantitative fluorogenic RT-PCR assay. Low levels of viral RNA were detected in lymph nodes in all groups 1 day after infection. However, at day 2, both $RL^{-/-}$ and $PKR^{-/-} \times RL^{-/-}$ mice averaged fourfold-higher levels of WNV RNA than wild-type mice ($P = 0.04$) (Fig. 2A). These data suggest that PKR and RNase L limit viral replication in the lymph node at early time points.

(ii) Viremia. WNV RNA was detected in the sera of wild-type, $RL^{-/-}$, and $PKR^{-/-} \times RL^{-/-}$ mice beginning on day 1 after infection by quantitative fluorogenic RT-PCR and peaked in all groups on day 3 after infection. In wild-type mice, WNV RNA levels subsequently decreased on day 4 and largely approached the limit of detection by day 6. However, $PKR^{-/-} \times RL^{-/-}$ mice showed a somewhat delayed clearance of viral RNA from their sera, with statistically higher levels of viral RNA on day 4 than in wild-type mice ($10^{2.5}$ viral copies/ml versus $10^{1.4}$ viral copies/ml, respectively; $P = 0.003$) (Fig. 2B). Thus, higher levels of circulating WNV were detected in PKR- and RNase L-deficient mice, and this finding correlated kinetically with the observed earlier entry of WNV into the CNS.

(iii) Spleen. Infectious WNV was detected by plaque assay at equivalent levels in the spleens of $RL^{-/-}$, $PKR^{-/-} \times RL^{-/-}$, and wild-type mice beginning on day 3 after infection. By day 4, however, only 66% (six of nine) of the wild-type mice had viral loads above the limit of detection, whereas 88% (seven of eight) of the $RL^{-/-}$ and 100% (eight of eight) of the $PKR^{-/-}$

$\times RL^{-/-}$ mice showed splenic infection. Consistent with this, $PKR^{-/-} \times RL^{-/-}$ mice had significantly higher viral burdens at day 4 than wild-type mice ($10^{4.7}$ PFU/g versus $10^{3.6}$ PFU/g, respectively; $P < 0.05$) (Fig. 2C). Despite the increased level of WNV in the spleens of $PKR^{-/-} \times RL^{-/-}$ mice, virus was cleared with similar kinetics in all groups of mice, and infectious virus was no longer detectable by day 8 after infection.

(iv) Type I IFN production. In addition to other molecules (e.g., TLR3 and RIG-I [1, 79]), PKR acts as an intracellular sensor for dsRNA and has been linked to type I IFN production in some cell types (10, 31, 41, 50). To determine if an altered production of type I IFN in $PKR^{-/-} \times RL^{-/-}$ mice contributed to the observed increase in peripheral viral burden, we compared IFN levels in sera on days 1 to 5 after infection using an EMCV bioassay of L929 cells. Notably, no significant differences in the serum levels of type I IFN-mediated protection were detected between wild-type and $PKR^{-/-} \times RL^{-/-}$ mice ($P \geq 0.1$) (Fig. 2D).

(v) WNV-specific IgM production. The induction of specific, neutralizing immunoglobulin M (IgM) early in the course of WNV infection has been shown to limit viremia and the spread to CNS tissues (15). Since one in vitro study suggested that PKR may regulate the transcriptional activation of immunoglobulin κ (light chain) (40), we evaluated whether $PKR^{-/-} \times RL^{-/-}$ mice had altered levels of WNV-specific IgM early in infection. Sera were harvested on day 4 after infection and analyzed for WNV-specific IgM levels. This day was chosen because differences in IgM response at day 4 correlate with changes in clinical phenotype (15). No significant difference ($P = 0.6$) was found in the levels of production of WNV-specific IgM between wild-type and $PKR^{-/-} \times RL^{-/-}$ mice, suggesting that the increased levels of WNV observed in peripheral compartments was not due to the altered production of WNV-specific IgM (Fig. 2E).

PKR and RNase L modulate cellular infection in the spleen. Type I IFN modulates the tropism of WNV at a cellular level, as mice lacking the type I IFN receptor showed higher spleen viral burdens that reflected increased infection in bone marrow-derived cell populations (62). Since $PKR^{-/-} \times RL^{-/-}$ mice also showed increased infection in the spleen, we tested whether PKR and RNase L altered viral infection in specific cell populations. Spleens were harvested from wild-type, $PKR^{-/-} \times RL^{-/-}$, and $RL^{-/-}$ mice on day 4 after infection, and $CD11c^+$, $CD11b^+$, and $CD19^+$ cell populations were isolated by positive selection with antibody-coated magnetic beads. Following RNA isolation, strand-specific, quantitative fluorogenic RT-PCR was performed to assess the levels of WNV positive- and negative-sense RNA. Increased levels of WNV positive-strand RNA were detected in $CD11b^+$, $CD11c^+$, and $CD19^+$ cells isolated from $PKR^{-/-} \times RL^{-/-}$ mice (295-, 127-, and 82-fold increases, respectively, relative to levels in wild-type mice; $P < 0.03$) (Fig. 3A and B and data not shown). Higher levels of positive-strand RNA were also detected in cell populations of $RL^{-/-}$ mice (50-, 6-, and 43-fold increases in $CD11b^+$, $CD11c^+$, and $CD19^+$ cells, respectively; $P < 0.04$), although levels were lower than those detected in $PKR^{-/-} \times RL^{-/-}$ mice. WNV negative strand, a direct marker of active viral replication, was detected in $CD11b^+$ cells isolated from $PKR^{-/-} \times RL^{-/-}$ mice, but the level was below the sensitivity of the assay in other tested cell popula-
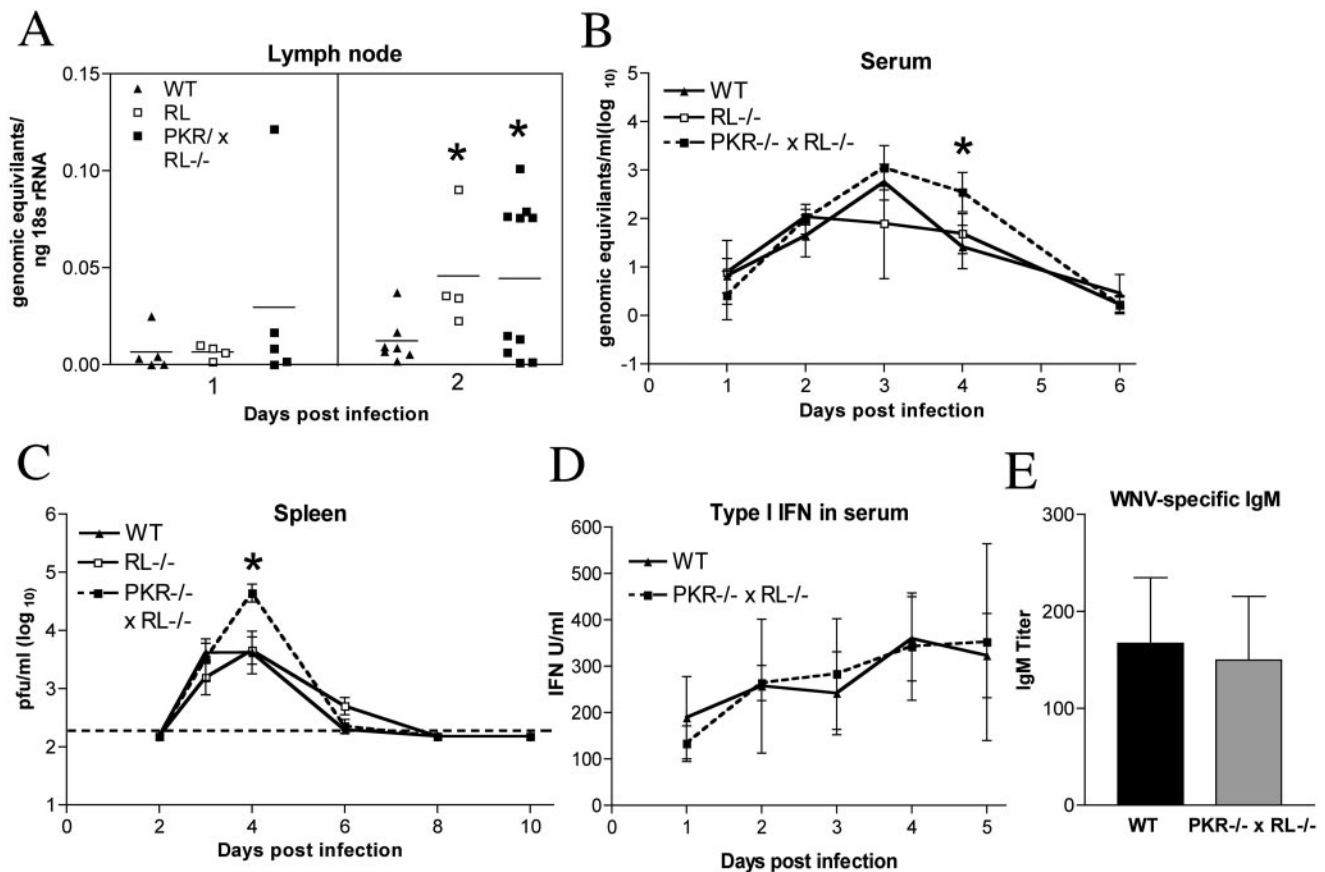
FIG. 2. PKR$^{-/-}$ × RL$^{-/-}$ mice show increased viral replication in the periphery. (A to C) Viral burdens in the lymph nodes, sera, and spleens of wild-type (WT), RL$^{-/-}$, and PKR$^{-/-}$ × RL$^{-/-}$ mice following footpad infection with 10^2 PFU of WNV. (A) Levels of viral RNA were measured from inguinal lymph nodes ipsilateral to the site of infection by quantitative RT-PCR. Data are shown as the genomic equivalents of WNV RNA per ng of 18S rRNA. (B) Viral RNA levels in sera were analyzed via quantitative RT-PCR. Data shown are genomic equivalents of WNV RNA per milliliter of serum. (C) WNV burden in the spleen was measured by plaque assay using samples harvested on the indicated days and is expressed as PFU per gram of tissue. The dotted line represents the limit of sensitivity of the assay. (D) Type I IFN concentrations were determined from sera collected on days 1 to 5 after infection by using an EMCV bioassay in L929 cells. Data reflect the averages from serum samples harvested from three to five mice per time point and are shown as units of IFN/ml of serum. (E) WNV-specific IgM levels were determined from sera collected on day 4 postinfection by enzyme-linked immunosorbent assay against purified recombinant WNV E protein. Data represent the averages from samples harvested from eight mice per group and are expressed as units of optical density after subtraction of the background. Error bars indicate the standard deviations, and asterisks indicate values that are statistically significant ($P < 0.05$) compared to those for wild-type mice in all panels.

tions from all groups of mice. These data suggest that the lack of PKR and RNase L directly affects infection by WNV in the spleen and that replication in CD11b$^+$ bone marrow-derived cells is enhanced.

To test directly whether PKR and RNase L contribute to IFN-mediated inhibition of WNV replication in myeloid cells, we generated BM-Mϕ and BM-DCs from C57BL/6 wild-type and congenic PKR$^{-/-}$ × RL$^{-/-}$ and RL$^{-/-}$ mice. Pretreatment of wild-type BM-Mϕ and BM-DCs with IFN-β reduced WNV replication to similar levels (10^4- to 10^5-fold inhibition). Small but significant decreases in IFN-β-mediated inhibition of WNV infection were detected in RL$^{-/-}$ and PKR$^{-/-}$ × RL$^{-/-}$ BM-Mϕs (three- and sixfold reduction, respectively; $P \leq 0.002$) (Fig. 3C). In contrast, the IFN-β-mediated inhibition of WNV in BM-DCs appeared to be independent of PKR and RNase L ($P \geq 0.1$) (Fig. 3D). Moreover, RL$^{-/-}$ and PKR$^{-/-}$ × RL$^{-/-}$ BM-Mϕs supported WNV replication more

efficiently than wild-type BM-Mϕs at 24 h postinfection ($P \leq 0.002$) (Fig. 3E), whereas no significant difference in the levels of viral growth in BM-DCs was observed (Fig. 3F). IFN-γ pretreatment of wild-type BM-Mϕs and BM-DCs also inhibited WNV replication, although BM-DCs responded less efficiently than BM-Mϕs to this cytokine (10^3-fold versus 10^1-fold inhibition). Additionally, while PKR and RNase L were not required for the IFN-γ-induced restriction of WNV in BM-Mϕs, a small but significant decrease in IFN-γ-mediated inhibition of WNV was observed in PKR$^{-/-}$ × RL$^{-/-}$ BM-DCs (sixfold reduction; $P = 0.0001$). Together, these experiments suggest that PKR and RNase L contribute to IFN-induced protection in a subset of bone marrow-derived cells in vivo and in vitro.

PKR and RNase L do not control mortality after IC infection. In addition to controlling the dissemination of WNV, type I IFN plays an independent role in limiting WNV replication in
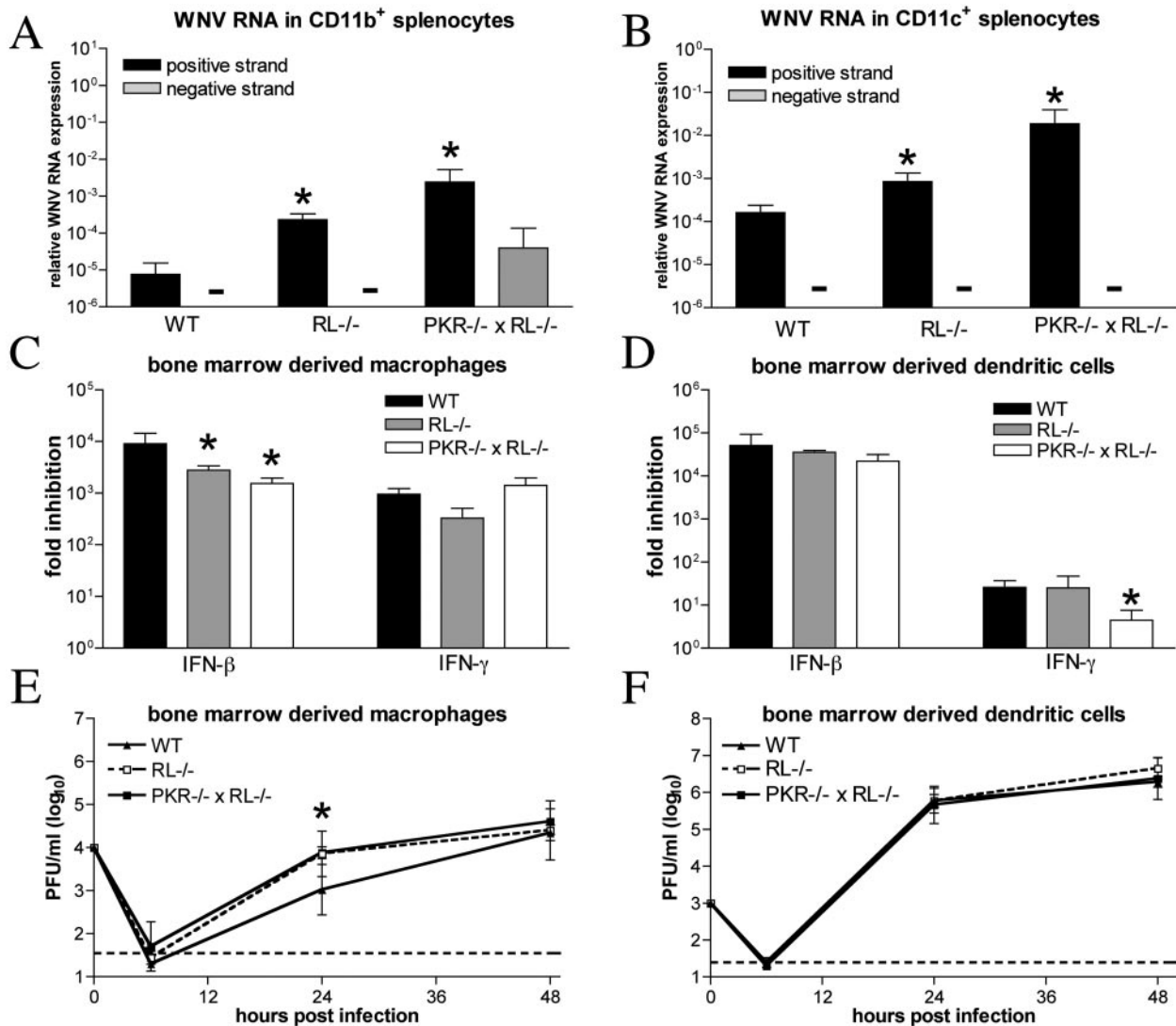
FIG. 3. PKR and RNase L modulate viral infection in bone marrow-derived cells. (A and B) Total RNA from CD11b$^+$ (A) and CD11c$^+$ (B) splenocytes isolated on day 4 postinfection was analyzed for the levels of WNV positive and negative strands with strand-specific real-time RT-PCR. Data are expressed as the amounts of positive- and negative-strand RNA relative to 18S rRNA levels. Average values are from four to eight mice per group. BM-Mφ (C) and BM-DCs (D) were generated from wild-type, RL$^{-/-}$, and PKR$^{-/-}$ × RL$^{-/-}$ mice and treated for 24 h with 1,000 IU/ml of mouse IFN-β or -γ prior to infection with an MOI of 0.1. The production of infectious virus at 24 h postinfection was determined by plaque assay. Average values represent results from quadruplicate samples harvested from three independent experiments. BM-Mφ (E) and BM-DCs (F) generated from wild-type, RL$^{-/-}$, and PKR$^{-/-}$ × RL$^{-/-}$ mice were infected at an MOI of 0.01, and viral production was evaluated at the indicated times postinfection by plaque assay. Values are averages of results from quadruplicate samples generated from two independent experiments, and asterisks indicate differences that are statistically significant relative to results for wild-type mice ($P < 0.05$).

CNS tissues directly (62). To test whether PKR and RNase L mediated this effect, we inoculated wild-type, RL$^{-/-}$, PKR$^{-/-}$ × RL$^{-/-}$, and IFN-α/βR$^{-/-}$ C57BL/6 mice with 10^1 PFU WNV via the IC route and monitored their survival. All groups of mice showed rapid and nearly complete mortality following IC infection. Similar to results observed in 129Sv/Ev mice (62), IFN-α/βR$^{-/-}$ C57BL/6 mice showed a marked vulnerability, with a mean time to death of 3.1 ± 0.1 days compared to 7.3 ± 1.2 days for wild-type mice ($P < 0.0001$). In contrast, the survival curves for wild-type, RL$^{-/-}$, and PKR$^{-/-}$ × RL$^{-/-}$ mice were virtually identical ($P > 0.2$) (Fig. 4A). These experiments suggest that PKR- and RNase L-independent antiviral

effector mechanisms function downstream of type I IFN to control WNV-induced mortality after IC infection.

PKR and RNase L control viral replication and spread following IC inoculation. Given the high degree of neurovirulence of the lineage I New York 2000 strain used in these studies, a mortality analysis alone after IC inoculation may not be sensitive enough to detect differences in CNS infection and spread. To address this, the viral burden was measured in the CNS and peripheral tissues of wild-type, RL$^{-/-}$, and PKR$^{-/-}$ × RL$^{-/-}$ mice on days 2, 4, and 6 after IC inoculation. Interestingly, the average viral burden in the brains of PKR$^{-/-}$ × RL$^{-/-}$ mice was 10-fold higher than in wild-type mice on day
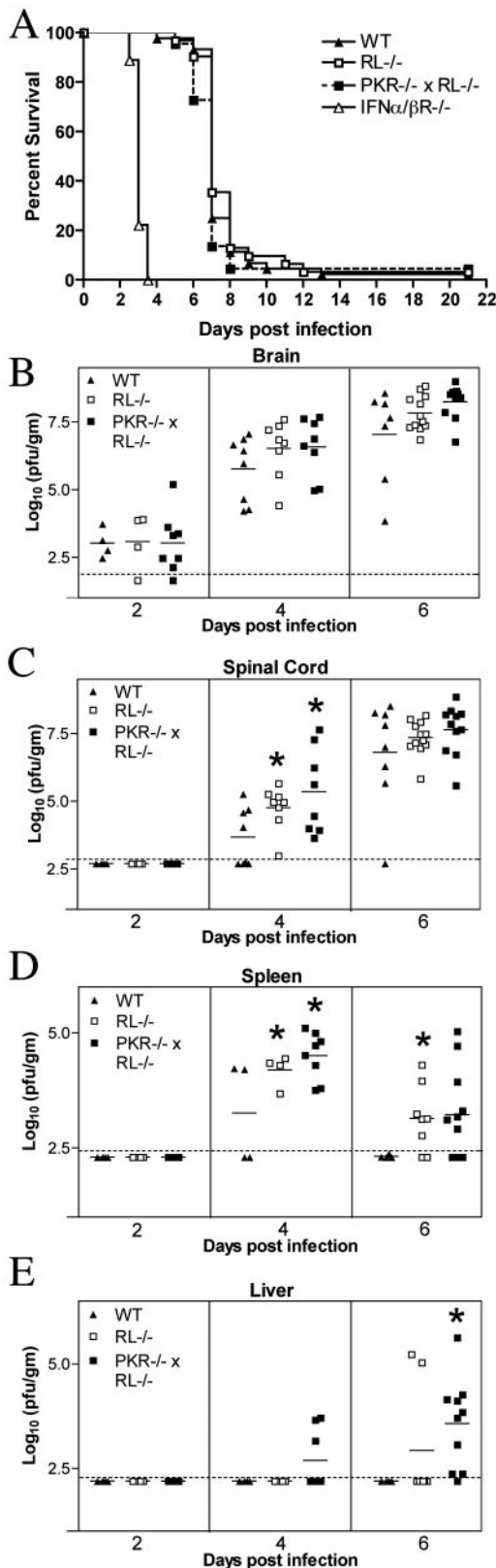
FIG. 4. Survival and viral burden data for wild-type (WT), RL$^{-/-}$, PKR$^{-/-}$ × RL$^{-/-}$, and IFN-α/βR$^{-/-}$ C57BL/6 mice after intracranial inoculation with 10^1 PFU of WNV. (A) Data from two to three independent experiments were used to construct the survival curves, for which 44 wild-type, 31 RL$^{-/-}$, 22 PKR$^{-/-}$ × RL$^{-/-}$, and 9 IFN-α/

6 ($10^{8.2}$ PFU/g versus $10^{7.0}$ PFU/g) (Fig. 4B). As anticipated because of the requirement for time-dependent spread, infectious virus was not detected in the spinal cord on day 2 after IC infection in any group. By day 4, 50% (four of eight) of the wild-type mice had measurable loads of virus in their spinal cords, with an average of $10^{3.7}$ PFU/g. At this time point, 100% (eight of eight) of both the RL$^{-/-}$ and the PKR$^{-/-}$ × RL$^{-/-}$ mice had infectious virus in their spinal cords, with higher viral burdens ($10^{4.7}$ PFU/g and $10^{5.5}$ PFU/g, respectively, compared to $10^{3.7}$ PFU/g in wild-type mice; $P < 0.04$) (Fig. 4C). At day 6, increased viral loads in the spinal cord again were detected in mice lacking both PKR and RNase L. These data suggest that PKR and RNase L contribute to the control of WNV replication in CNS tissues directly.

Although intracranial infection of WNV results in rapid, overwhelming replication in the brain and spinal cord, viral spread to peripheral tissues also can occur. Since PKR and RNase L restricted viral infection in specific cell populations in the spleen, we evaluated whether these effector proteins modulated WNV spread following IC infection. Fifty percent of wild-type mice (two of four) had infectious virus in the spleen beginning on day 4 after infection; WNV was completely cleared by day 6, despite increasing CNS titers. In comparison, all RL$^{-/-}$ (four of four) and PKR$^{-/-}$ × RL$^{-/-}$ mice (eight of eight) had infectious virus in their spleens on day 4, with significantly higher viral loads than those in wild-type mice ($10^{6.5}$ PFU/g and $10^{6.6}$ PFU/g, respectively, versus $10^{5.7}$ PFU/g in wild-type mice; $P \leq 0.03$) (Fig. 4D). Additionally, an attenuated clearance from the spleen was observed in RL$^{-/-}$ and PKR$^{-/-}$ × RL$^{-/-}$ mice, with detectable virus at day 6 postinfection in 75% (6 of 8) and 64% (7 of 11) of spleens of RL$^{-/-}$ and PKR$^{-/-}$ × RL$^{-/-}$ mice, respectively. Although the spleen is a normal target for WNV infection in multiple infection models (14, 53, 66), WNV replication is not consistently detected in other peripheral nonlymphoid organs. However, mice lacking the type I IFN receptor showed an expanded WNV tropism in peripheral tissues (62). To assess whether a lack of PKR and RNase L also modulated WNV tropism, viral burden in the liver was evaluated after IC infection. Consistent with our findings after subcutaneous infection (14), infectious WNV was not detected in the livers of wild-type mice at any time point. However, PKR$^{-/-}$ × RL$^{-/-}$ mice developed hepatic infection beginning on day 4 (Fig. 4E), and by day 6 after infection, 90% (9 of 10) of PKR$^{-/-}$ × RL$^{-/-}$ mice and 25% (2 of 8) RL$^{-/-}$ mice had measurable levels of virus in their livers, with an average of $10^{3.6}$ PFU/g. Thus, deficiencies in PKR and RNase L resulted in an altered viral tropism at a tissue level.

βR$^{-/-}$ mice were used. The mean times to death for wild-type, RL$^{-/-}$, and PKR$^{-/-}$ × RL$^{-/-}$ mice were not statistically different, whereas the mean time to death for IFN-α/βR$^{-/-}$ mice was significantly decreased ($P < 0.0001$). (B through E) Viral burden in tissues after intracranial WNV infection. Viral loads in brain (B), spinal cord (C), spleen (D), and liver (E) were measured by plaque assay from samples harvested on days 2, 4, and 6 after infection and reflect results for four to eight mice per group. The dotted line represents the limit of sensitivity of the assay, and asterisks indicate values that are statistically significant ($P < 0.05$) compared to those for wild-type mice.
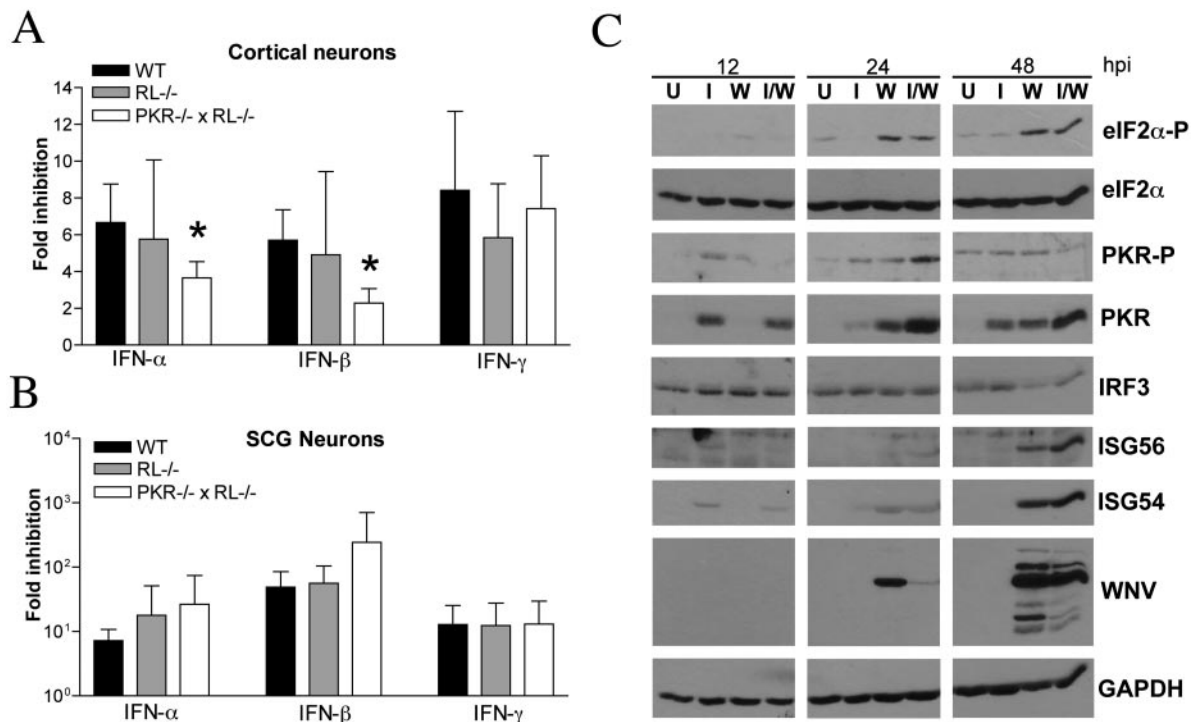
FIG. 5. Effects of PKR and RNase L on IFN-mediated inhibition of WNV infection in neurons. (A and B) Primary cultures of cortical and SCG neurons were prepared from wild-type, $RL^{-/-}$, and $PKR^{-/-}RL^{-/-}$ mice. Cortical neurons (A) or SCG neurons (B) were treated 24 h prior to infection with 100 IU/ml of the indicated mouse IFN. Neurons were infected with WNV and evaluated for the production of infectious virus at 24 h by a plaque assay. Data represent averages of results from three to five independent experiments, and asterisks indicate values that are statistically significant ($P < 0.05$) compared to those for treated wild-type cells. (C) Whole-cell lysates were generated at the indicated times (hours postinfection [hpi]) from cortical neurons that were uninfected (lanes U), infected with WNV at an MOI of 0.1 (lanes W), treated with IFN-β at 100 IU/ml (lanes I), or infected with WNV and treated with IFN at the time of infection (lanes I/W). Protein levels of phosphorylated PKR (PKR-P), phosphorylated eIF2-α (eIF2α-P), total PKR, total eIF2-α, mouse IRF-3, ISG56, ISG54, WNV, and GAPDH were examined by immunoblot analysis.

PKR and RNase L act as IFN-activated antiviral effector proteins in cortical neurons. Although in vivo studies suggested that PKR and RNase L modulate viral replication in CNS tissues (Fig. 4), their direct role in inhibiting viral infection in neurons remained unclear. To assess whether PKR and RNase L mediated the antiviral effects of IFN in CNS-derived neurons, we infected wild-type and congenic $RL^{-/-}$ and $PKR^{-/-} \times RL^{-/-}$ primary cortical neurons in the presence or absence of IFN pretreatment. Cortical neurons were used because this neuronal subtype is infected in human and animal cases of WNV encephalitis (14, 55, 76). Pretreatment with IFN-α, -β, or -γ reduced WNV infection 8- to 15-fold in wild-type cortical neurons. A decrease in IFN-α- and IFN-β-mediated inhibition of WNV infection was observed in $PKR^{-/-} \times RL^{-/-}$ neurons (two- and threefold reduction, respectively; $P \leq 0.02$) (Fig. 5A). To test whether the antiviral roles of PKR and RNase L varied among neuronal subtypes, SCG peripheral nervous system sympathetic motor neurons were generated from wild-type and congenic $RL^{-/-}$ and $PKR^{-/-} \times RL^{-/-}$ mice and infected with WNV with and without IFN pretreatment. In contrast to cortical neurons, SCG neurons lacking PKR and RNase L showed no significant decrease in the inhibition of WNV following treatment with IFN-α or IFN-β ($P \geq 0.2$) (Fig. 5B). Thus, while PKR and RNase L contribute to the antiviral effects of type I IFN in cortical neurons, independent effector molecules may play dominant antiviral roles

in other neuronal subtypes. To confirm that the PKR activation pathway was functional in cortical neurons and begin to evaluate other downstream targets of type I IFN in this cell type, we performed Western blot analyses of cortical neuron lysates generated from WNV-infected and IFN-β-treated cells (Fig. 5C). PKR was detectable at 12 h after IFN treatment and throughout the infection time course. Importantly, PKR phosphorylation was associated with a reduction in the steady-state levels of viral protein, and phosphorylated PKR and phosphorylated eIF2-α were detected 24 h sooner than ISG54 and ISG56 after WNV infection. Consistent with our virologic results, these data demonstrate that PKR is activated in cortical neurons in response to WNV infection.

DISCUSSION

In this study, we used several different experimental approaches to demonstrate that PKR and RNase L act as important effector molecules against WNV infection. Mice lacking PKR and RNase L were significantly more susceptible to WNV infection and showed increased viremia and viral burden in peripheral tissues, early entry into the brain, and higher viral loads in the CNS than wild-type mice. In vivo and in vitro studies suggest that CD11b$^+$ bone marrow-derived cells specifically utilize PKR and RNase L to modulate WNV replication. PKR- and RNase L-deficient mice also showed higher

viral burdens in CNS tissues following IC inoculation. Experiments in primary cortical neurons suggest that PKR and RNase L contribute to IFN-mediated protection against WNV, as genetically deficient neurons showed reduced sensitivity to the antiviral effects of type I IFN.

PKR and RNase L modulate WNV pathogenesis in mice. Although in vivo and in vitro studies have demonstrated that type I IFN limits WNV infection and spread (62), the IFN-induced antiviral molecules that control WNV infection remain unidentified. Our experiments show that PKR and RNase L contribute to the control of WNV replication in vivo, as increased lethality following peripheral inoculation was observed in $RL^{-/-}$ and $PKR^{-/-} \times RL^{-/-}$ mice. Nonetheless, RNase L-deficient mice were less susceptible than mice lacking both effector proteins, suggesting an additional protective role for PKR. PKR and RNase L together contribute to the control of WNV infection in the periphery, as enhanced viral burdens were observed in lymphoid tissues and sera of mice lacking both effectors. This increase in peripheral infection correlated with an earlier entry into the brain and higher CNS viral burdens. The change in peripheral replication and dissemination did not appear to be due to a defect in immune priming, as normal levels of type I IFN and WNV-specific IgM were induced. However, because type I IFN-α/β receptor-deficient mice showed a more severe phenotype than $PKR^{-/-} \times RL^{-/-}$ mice, additional, as-yet-undefined, IFN-activated effector molecules must also control WNV infection.

Though studies to date have not directly tested the role of PKR and RNase L in modulating flavivirus infection in vivo, components of the RNase L signaling pathway have been implicated in the control of WNV infection. WNV replicated to higher titers in RNase L-deficient MEFs, though this increase appeared to be independent of type I IFN (64). Additionally, a mutation in the 2′,5′-oligoadenylate synthetase 1b (*Oas1b*) gene that results in the expression of truncated Oas1b was correlated with WNV susceptibility in mice (51, 56). The overexpression of full-length but not truncated Oas1b in MEFs decreased WNV replication by reducing the accumulation of positive-strand RNA (34), and some single-nucleotide polymorphisms in OAS genes were found at a higher frequency in humans hospitalized for WNV infection (77). However, the mechanisms by which *Oas1b* alleles affect WNV pathogenesis remain unclear. Recent studies suggest that RNase L activation does not play a significant role in Oas1b-dependent resistance to flaviviruses. Levels of RNase L activation were comparable in cells derived from mice that expressed full-length and truncated *Oas1b* genes. Furthermore, RNase L inhibition or genetic deficiency resulted in similar increases in WNV replication in both *Oas1b*-sufficient and -deficient backgrounds (64). Our data support an Oas1b-independent mechanism for RNase L-mediated protection from WNV infection in vivo: the $RL^{-/-}$ and $PKR^{-/-} \times RL^{-/-}$ C57BL/6 mice used in this study express the truncated form of the *Oas1b* gene.

The experiments described here are consistent with prior in vivo investigations of other DNA and RNA viruses. RNase L-deficient mice had increased lethality following encephalomyocarditis virus infection in both the presence and absence of IFN-α pretreatment (81). Similarly, mice lacking PKR or RNase L had significantly increased lethality following infection with coxsackievirus (20), and $PKR^{-/-}$ mice also showed

increased lethality following VSV infection (16, 71). In contrast, $PKR^{-/-} \times RL^{-/-}$ mice showed no increase in morbidity or mortality following subcutaneous infection with Sindbis alphavirus, although higher viral loads were observed in draining lymph nodes (60). While the contribution of PKR and RNase L to IFN-induced protection appears to vary among viral families, our data suggest that these effector proteins can significantly modulate the severity and outcome of WNV infection.

PKR and RNase L have cell-restricted roles in modulating WNV infection. Previous experiments demonstrated that type I IFN limits WNV replication in several cell populations in vivo and in vitro, with bone marrow-derived cells and neurons showing markedly altered infection patterns in the absence of IFN-mediated protection (62). Our current study begins to elucidate which antiviral effector proteins downstream of IFN affect WNV infection. We observed increased levels of infectious WNV in type I IFN-α/β receptor-deficient mice that were similar to those observed in both the spleens and livers of $PKR^{-/-} \times RL^{-/-}$ mice. Higher levels of positive-strand RNA were detected in $CD11b^+$, $CD11c^+$, and $CD19^+$ cells derived from the spleens of $PKR^{-/-} \times RL^{-/-}$ and $RL^{-/-}$ mice. Negative-strand viral RNA, the replicative intermediate of WNV, however, was measurable only in $CD11b^+$ cells from $PKR^{-/-} \times RL^{-/-}$ mice. Our in vitro data supported the hypothesis that PKR and RNase L restrict WNV replication in $CD11b^+$ cells: type I IFN-mediated inhibition of WNV was partially dependent on PKR and RNase L in BM-Mϕs, and this phenotype was associated with increased replication in BM-Mϕs lacking both effector molecules. In contrast, responsiveness to type I IFN appeared intact in PKR- and RNase L-deficient BM-DCs. We did observe a slight decrease in the ability of $PKR^{-/-} \times RL^{-/-}$ BM-DCs to inhibit WNV in response to IFN-γ, although this phenotype was not associated with increased WNV replication in a multistep growth curve analysis. These data suggest that type I IFN limits WNV replication in $CD11b^+$ cells in the spleen in part through the antiviral activities of PKR and RNase L but that additional IFN-simulated genes likely play dominant inhibitory roles in other spleen cell populations.

In addition to conferring protection to bone marrow-derived cells, our experiments suggest that PKR and RNase L mediate the antiviral effects of IFN directly in the CNS. Although mice lacking PKR and RNase L did not show enhanced lethality after IC infection, higher CNS viral burdens were observed. Consistent with this, PKR and RNase L partially mediated the antiviral effects of type I IFN in cortical neurons. The PKR pathway was rapidly activated in cortical neurons by WNV infection, and this occurred 24 h prior to the induction of other ISGs. We speculate that PKR may restrict WNV replication in cortical neurons prior to the production of other antiviral proteins, an idea consistent with the ability of PKR to mediate eIF2-α-dependent translational shutoff (35, 61, 74). In contrast, PKR and RNase L did not appear to mediate the antiviral effects of type I IFN in SCG sympathetic motor neurons of peripheral origin.

Our studies suggest that PKR and RNase L mediate the IFN inhibition of WNV in some cell populations but are dispensable for the control of infection in others. Analogously, different cell types have shown varied requirements for PKR and RNase L in the context of other viral infections. Although

the interferon responsiveness of PKR$^{-/-}$ $\times$ RL$^{-/-}$ MEFs or BM-DCs was largely intact in the context of DENV or WNV infection (13, 64), MEFs deficient in PKR showed a decreased IFN-mediated inhibition of VSV (71). Moreover, our results agree with prior reports that showed that PKR and RNase L were important for IFN-β-mediated resistance to HSV type 1 in trigeminal ganglion cultures (2) but that PKR was dispensable for the IFN-γ-mediated inhibition of vesicular stomatitis virus in neuroblastoma cells (12). We postulate a model in which distinct cell types differentially utilize PKR and RNase L to inhibit viral infection. This variable requirement for PKR and RNase L suggests that cell-specific antiviral programs that may differ in both the kinetics and repertoire of IFN-induced antiviral proteins are induced by IFN. To this end, genetic profiling studies are under way to identify novel cell-specific IFN-induced antiviral pathways that inhibit WNV.

ACKNOWLEDGMENTS

References

1. **Alexopoulou, L., A. C. Holt, R. Medzhitov, and R. A. Flavell.** 2001. Recognition of double-stranded RNA and activation of NF-kappaB by Toll-like receptor 3. Nature **413:**732–738.
2. **Al-khatib, K., B. R. Williams, R. H. Silverman, W. Halford, and D. J. Carr.** 2003. The murine double-stranded RNA-dependent protein kinase PKR and the murine 2′,5′-oligoadenylate synthetase-dependent RNase L are required for IFN-beta-mediated resistance against herpes simplex virus type 1 in primary trigeminal ganglion culture. Virology **313:**126–135.
3. **Asnis, D. S., R. Conetta, A. A. Teixeira, G. Waldman, and B. A. Sampson.** 2000. The West Nile virus outbreak of 1999 in New York: the Flushing Hospital experience. Clin. Infect. Dis. **30:**413–418.
4. **Austin, B. A., C. James, R. H. Silverman, and D. J. Carr.** 2005. Critical role for the oligoadenylate synthetase/RNase L pathway in response to IFN-beta during acute ocular herpes simplex virus type 1 infection. J. Immunol. **175:**1100–1106.
5. **Balachandran, S., P. C. Roberts, L. E. Brown, H. Truong, A. K. Pattnaik, D. R. Archer, and G. N. Barber.** 2000. Essential role for the dsRNA-dependent protein kinase PKR in innate immunity to viral infection. Immunity **13:**129–141.
6. **Byrne, S. N., G. M. Halliday, L. J. Johnston, and N. J. King.** 2001. Interleukin-1beta but not tumor necrosis factor is involved in West Nile virus-induced Langerhans cell migration from the skin in C57BL/6 mice. J. Investig. Dermatol. **117:**702–709.
7. **Carr, D. J., K. Al-khatib, C. M. James, and R. Silverman.** 2003. Interferon-beta suppresses herpes simplex virus type 1 replication in trigeminal ganglion cells through an RNase L-dependent pathway. J. Neuroimmunol. **141:**40–46.
8. **Ceausu, E., S. Erscoiu, P. Calistru, D. Ispas, O. Dorobat, M. Homos, C. Barbulescu, I. Cojocaru, C. V. Simion, C. Cristea, C. Oprea, C. Dumitrescu, D. Duiculescu, I. Marcu, C. Mociornita, T. Stoicev, I. Zolotusca, C. Calomfirescu, R. Rusu, R. Hodrea, S. Geamai, and L. Paun.** 1997. Clinical manifestations in the West Nile virus outbreak. Rom. J. Virol. **48:**3–11.
9. **Celada, A., P. W. Gray, E. Rinderknecht, and R. D. Schreiber.** 1984. Evidence for a gamma-interferon receptor that regulates macrophage tumoricidal activity. J. Exp. Med. **160:**55–74.
10. **Ceppi, M., N. Ruggli, V. Tache, H. Gerber, K. C. McCullough, and A. Summerfield.** 2005. Double-stranded secondary structures on mRNA induce type I interferon (IFN alpha/beta) production and maturation of mRNA-transfected monocyte-derived dendritic cells. J. Gene Med. **7:**452–465.
11. **Chambers, T. J., and M. S. Diamond.** 2003. Pathogenesis of flavivirus encephalitis. Adv. Virus Res. **60:**273–342.
12. **Chesler, D. A., J. L. Munoz-Jordan, N. Donelan, A. Garcia-Sastre, and C. S. Reiss.** 2003. PKR is not required for interferon-gamma inhibition of VSV replication in neurons. Viral Immunol. **16:**87–96.
13. **Diamond, M. S., and E. Harris.** 2001. Interferon inhibits dengue virus infection by preventing translation of viral RNA through a PKR-independent mechanism. Virology **289:**297–311.

14. **Diamond, M. S., B. Shrestha, A. Marri, D. Mahan, and M. Engle.** 2003. B cells and antibody play critical roles in the immediate defense of disseminated infection by West Nile encephalitis virus. J. Virol. **77:**2578–2586.
15. **Diamond, M. S., E. M. Sitati, L. D. Friend, S. Higgs, B. Shrestha, and M. Engle.** 2003. A critical role for induced IgM in the protection against West Nile virus infection. J. Exp. Med. **198:**1853–1862.
16. **Durbin, R. K., S. E. Mertz, A. E. Koromilas, and J. E. Durbin.** 2002. PKR protection against intranasal vesicular stomatitis virus infection is mouse strain dependent. Viral Immunol. **15:**41–51.
17. **Easton, R. M., T. L. Deckwerth, A. S. Parsadanian, and E. M. Johnson, Jr.** 1997. Analysis of the mechanism of loss of trophic factor dependence associated with neuronal maturation: a phenotype indistinguishable from Bax deletion. J. Neurosci. **17:**9656–9666.
18. **Ebel, G. D., A. P. Dupuis III, K. Ngo, D. Nicholas, E. Kauffman, S. A. Jones, D. Young, J. Maffei, P. Y. Shi, K. Bernard, and L. D. Kramer.** 2001. Partial genetic characterization of West Nile virus strains, New York State, 2000. Emerg. Infect. Dis. **7:**650–653.
19. **Eldadah, A. H., and N. Nathanson.** 1967. Pathogenesis of West Nile Virus encephalitis in mice and rats. II. Virus multiplication, evolution of immunofluorescence, and development of histological lesions in the brain. Am. J. Epidemiol. **86:**776–790.
20. **Flodstrom-Tullberg, M., M. Hultcrantz, A. Stotland, A. Maday, D. Tsai, C. Fine, B. Williams, R. Silverman, and N. Sarvetnick.** 2005. RNase L and double-stranded RNA-dependent protein kinase exert complementary roles in islet cell defense during coxsackievirus infection. J. Immunol. **174:**1171–1177.
21. **Fratkin, J. D., A. A. Leis, D. S. Stokic, S. A. Slavinski, and R. W. Geiss.** 2004. Spinal cord neuropathology in human West Nile virus infection. Arch. Pathol. Lab. Med. **128:**533–537.
22. **Fredericksen, B. L., and M. Gale, Jr.** 2006. West Nile virus evades activation of interferon regulatory factor 3 through RIG-I-dependent and -independent pathways without antagonizing host defense signaling. J. Virol. **80:**2913–2923.
23. **Fredericksen, B. L., M. Smith, M. G. Katze, P. Y. Shi, and M. Gale, Jr.** 2004. The host response to West Nile virus infection limits viral spread through the activation of the interferon regulatory factor 3 pathway. J. Virol. **78:**7737–7747.
24. **Gale, M., Jr., B. Kwieciszewski, M. Dossett, H. Nakao, and M. G. Katze.** 1999. Antiapoptotic and oncogenic potentials of hepatitis C virus are linked to interferon resistance by viral repression of the PKR protein kinase. J. Virol. **73:**6506–6516.
25. **Glass, W. G., J. K. Lim, R. Cholera, A. G. Pletnev, J. L. Gao, and P. M. Murphy.** 2005. Chemokine receptor CCR5 promotes leukocyte trafficking to the brain and survival in West Nile virus infection. J. Exp. Med. **202:**1087–1098.
26. **Glass, W. G., D. H. McDermott, J. K. Lim, S. Lekhong, S. F. Yu, W. A. Frank, J. Pape, R. C. Cheshier, and P. M. Murphy.** 2006. CCR5 deficiency increases risk of symptomatic West Nile virus infection. J. Exp. Med. **203:**35–40.
27. **Gomez, C. E., A. M. Vandermeeren, M. A. Garcia, E. Domingo-Gil, and M. Esteban.** 2005. Involvement of PKR and RNase L in translational control and induction of apoptosis after hepatitis C polyprotein expression from a vaccinia virus recombinant. Virol. J. **2:**81.
28. **Gorchakov, R., E. Frolova, B. R. G. Williams, C. M. Rice, and I. Frolov.** 2004. PKR-dependent and -independent mechanisms are involved in translational shutoff during Sindbis virus infection. J. Virol. **78:**8455–8467.
29. **Granwehr, B. P., K. M. Lillibridge, S. Higgs, P. W. Mason, J. F. Aronson, G. A. Campbell, and A. D. Barrett.** 2004. West Nile virus: where are we now? Lancet Infect. Dis. **4:**547–556.
30. **Guo, J. T., J. Hayashi, and C. Seeger.** 2005. West Nile virus inhibits the signal transduction pathway of alpha interferon. J. Virol. **79:**1343–1350.
31. **Hornung, V., J. Schlender, M. Guenthner-Biller, S. Rothenfusser, S. Endres, K. K. Conzelmann, and G. Hartmann.** 2004. Replication-dependent potent IFN-alpha induction in human plasmacytoid dendritic cells by a single-stranded RNA virus. J. Immunol. **173:**5935–5943.
32. **Huhn, G. D., C. Austin, C. Langkop, K. Kelly, R. Lucht, R. Lampman, R. Novak, L. Haramis, R. Boker, S. Smith, M. Chudoba, S. Gerber, C. Conover, and M. S. Dworkin.** 2005. The emergence of West Nile virus during a large outbreak in Illinois in 2002. Am. J. Trop. Med. Hyg. **72:**768–776.
33. **Johnston, L. J., G. M. Halliday, and N. J. King.** 2000. Langerhans cells migrate to local lymph nodes following cutaneous infection with an arbovirus. J. Investig. Dermatol. **114:**560–568.
34. **Kajaste-Rudnitski, A., T. Mashimo, M. P. Frenkiel, J. L. Guenet, M. Lucas, and P. Despres.** 2006. The 2′,5′-oligoadenylate synthetase 1b is a potent inhibitor of West Nile virus replication inside infected cells. J. Biol. Chem. **281:**4624–4637.
35. **Katze, M. G.** 1995. Regulation of the interferon-induced PKR: can viruses cope? Trends Microbiol. **3:**75–78.
36. **Kerr, I. M., and R. E. Brown.** 1978. pppA2′p5′A2′p5′A: an inhibitor of protein synthesis synthesized with an enzyme fraction from interferon-treated cells. Proc. Natl. Acad. Sci. USA **75:**256–260.
37. **Khabar, K. S., M. Dhalla, Y. Siddiqui, A. Zhou, M. N. Al-Ahdal, S. D. Der, R. H. Silverman, and B. R. Williams.** 2000. Effect of deficiency of the

double-stranded RNA-dependent protein kinase, PKR, on antiviral resistance in the presence or absence of ribonuclease L: HSV-1 replication is particularly sensitive to deficiency of the major IFN-mediated enzymes. J. Interferon Cytokine Res. **20:**653–659.

38. **Klein, R. S., E. Lin, B. Zhang, A. D. Luster, J. Tollett, M. A. Samuel, M. Engle, and M. S. Diamond.** 2005. Neuronal CXCL10 directs CD8$^+$ T-cell recruitment and control of West Nile virus encephalitis. J. Virol. **79:**11457–11466.

39. **Kleinschmidt-DeMasters, B. K., B. A. Marder, M. E. Levi, S. P. Laird, J. T. McNutt, E. J. Escott, G. T. Everson, and K. L. Tyler.** 2004. Naturally acquired West Nile virus encephalomyelitis in transplant recipients: clinical, laboratory, diagnostic, and neuropathological features. Arch. Neurol. **61:**1210–1220.

40. **Koromilas, A. E., C. Cantin, A. W. Craig, R. Jagus, J. Hiscott, and N. Sonenberg.** 1995. The interferon-inducible protein kinase PKR modulates the transcriptional activation of immunoglobulin kappa gene. J. Biol. Chem. **270:**25426–25434.

41. **Kumar, A., J. Haque, J. Lacoste, J. Hiscott, and B. R. Williams.** 1994. Double-stranded RNA-dependent protein kinase activates transcription factor NF-kappa B by phosphorylating I kappa B. Proc. Natl. Acad. Sci. USA **91:**6288–6292.

42. **Lanciotti, R. S., A. J. Kerst, R. S. Nasci, M. S. Godsey, C. J. Mitchell, H. M. Savage, N. Komar, N. A. Panella, B. C. Allen, K. E. Volpe, B. S. Davis, and J. T. Roehrig.** 2000. Rapid detection of West Nile virus from human clinical specimens, field-collected mosquitoes, and avian samples by a TaqMan reverse transcriptase-PCR assay. J. Clin. Microbiol. **38:**4066–4071.

43. **Leis, A. A., J. Fratkin, D. S. Stokic, T. Harrington, R. M. Webb, and S. A. Slavinski.** 2003. West Nile poliomyelitis. Lancet Infect. Dis. **3:**9–10.

44. **Leis, A. A., D. S. Stokic, J. L. Polk, V. Dostrow, and M. Winkelmann.** 2002. A poliomyelitis-like syndrome from West Nile virus infection. N. Engl. J. Med. **347:**1279–1280.

45. **Li, X.-L., J. A. Blackford, and B. A. Hassel.** 1998. RNase L mediates the antiviral effect of interferon through a selective reduction in viral RNA during encephalomyocarditis virus infection. J. Virol. **72:**2752–2759.

46. **Lin, R.-J., C.-L. Liao, E. Lin, and Y.-L. Lin.** 2004. Blocking of the alpha interferon-induced Jak-Stat signaling pathway by Japanese encephalitis virus infection. J. Virol. **78:**9285–9294.

47. **Liu, W. J., X. J. Wang, D. C. Clark, M. Lobigs, R. A. Hall, and A. A. Khromykh.** 2006. A single amino acid substitution in the West Nile virus nonstructural protein NS2A disables its ability to inhibit alpha/beta interferon induction and attenuates virus virulence in mice. J. Virol. **80:**2396–2404.

48. **Liu, W. J., X. J. Wang, V. V. Mokhonov, P.-Y. Shi, R. Randall, and A. A. Khromykh.** 2005. Inhibition of interferon signaling by the New York 99 strain and Kunjin subtype of West Nile virus involves blockage of STAT1 and STAT2 activation by nonstructural proteins. J. Virol. **79:**1934–1942.

49. **Lobigs, M., A. Mullbacher, Y. Wang, M. Pavy, and E. Lee.** 2003. Role of type I and type II interferon responses in recovery from infection with an encephalitic flavivirus. J. Gen. Virol. **84:**567–572.

50. **Malmgaard, L., J. Melchjorsen, A. G. Bowie, S. C. Mogensen, and S. R. Paludan.** 2004. Viral activation of macrophages through TLR-dependent and -independent pathways. J. Immunol. **173:**6890–6898.

51. **Mashimo, T., M. Lucas, D. Simon-Chazottes, M. P. Frenkiel, X. Montagutelli, P. E. Ceccaldi, V. Deubel, J. L. Guenet, and P. Despres.** 2002. A nonsense mutation in the gene encoding 2′-5′-oligoadenylate synthetase/L1 isoform is associated with West Nile virus susceptibility in laboratory mice. Proc. Natl. Acad. Sci. USA **99:**11311–11316.

52. **Meurs, E. F., Y. Watanabe, S. Kadereit, G. N. Barber, M. G. Katze, K. Chong, B. R. G. Williams, and A. G. Hovanessian.** 1992. Constitutive expression of human double-stranded RNA-activated p68 kinase in murine cells mediates phosphorylation of eukaryotic initiation factor 2 and partial resistance to encephalomyocarditis virus growth. J. Virol. **66:**5805–5814.

53. **Morrey, J. D., C. W. Day, J. G. Julander, A. L. Olsen, R. W. Sidwell, C. D. Cheney, and L. M. Blatt.** 2004. Modeling hamsters for evaluating West Nile virus therapies. Antivir. Res. **63:**41–50.

54. **Munoz-Jordan, J. L., G. G. Sanchez-Burgos, M. Laurent-Rolle, and A. Garcia-Sastre.** 2003. Inhibition of interferon signaling by dengue virus. Proc. Natl. Acad. Sci. USA **100:**14333–14338.

55. **Omalu, B. I., A. A. Shakir, G. Wang, W. I. Lipkin, and C. A. Wiley.** 2003. Fatal fulminant pan-meningo-polioencephalitis due to West Nile virus. Brain Pathol. **13:**465–472.

56. **Perelygin, A. A., S. V. Scherbik, I. B. Zhulin, B. M. Stockman, Y. Li, and M. A. Brinton.** 2002. Positional cloning of the murine flavivirus resistance gene. Proc. Natl. Acad. Sci. USA **99:**9322–9327.

57. **Pestka, S., C. D. Krause, and M. R. Walter.** 2004. Interferons, interferon-like cytokines, and their receptors. Immunol. Rev. **202:**8–32.

58. **Pierson, T. C., M. S. Diamond, A. A. Ahmed, L. E. Valentine, C. W. Davis, M. A. Samuel, S. L. Hanna, B. A. Puffer, and R. W. Doms.** 2005. An infectious West Nile virus that expresses a GFP reporter gene. Virology **334:**28–40.

59. **Ryman, K. D., K. C. Meier, E. M. Nangle, S. L. Ragsdale, N. L. Korneeva, R. E. Rhoads, M. R. MacDonald, and W. B. Klimstra.** 2005. Sindbis virus

translation is inhibited by a PKR/RNase L-independent effector induced by alpha/beta interferon priming of dendritic cells. J. Virol. **79:**1487–1499.

60. **Ryman, K. D., L. J. White, R. E. Johnston, and W. B. Klimstra.** 2002. Effects of PKR/RNase L-dependent and alternative antiviral pathways on alphavirus replication and pathogenesis. Viral Immunol. **15:**53–76.

61. **Samuel, C. E.** 1998. Reoviruses and the interferon system. Curr. Top. Microbiol. Immunol. **233:**125–145.

62. **Samuel, M. A., and M. S. Diamond.** 2005. Alpha/beta interferon protects against lethal West Nile virus infection by restricting cellular tropism and enhancing neuronal survival. J. Virol. **79:**13350–13361.

63. **Sawicki, D. L., R. H. Silverman, B. R. Williams, and S. G. Sawicki.** 2003. Alphavirus minus-strand synthesis and persistence in mouse embryo fibroblasts derived from mice lacking RNase L and protein kinase R. J. Virol. **77:**1801–1811.

64. **Scherbik, S. V., J. M. Paranjape, B. M. Stockman, R. H. Silverman, and M. A. Brinton.** 2006. RNase L plays a role in the antiviral response to West Nile virus. J. Virol. **80:**2987–2999.

65. **Sejvar, J. J., M. B. Haddad, B. C. Tierney, G. L. Campbell, A. A. Marfin, J. A. Van Gerpen, A. Fleischauer, A. A. Leis, D. S. Stokic, and L. R. Petersen.** 2003. Neurologic manifestations and outcome of West Nile virus infection. JAMA **290:**511–515.

66. **Senne, D. A., J. C. Pedersen, D. L. Hutto, W. D. Taylor, B. J. Schmitt, and B. Panigrahy.** 2000. Pathogenicity of West Nile virus in chickens. Avian Dis. **44:**642–649.

67. **Shresta, S., J. L. Kyle, H. M. Snider, M. Basavapatna, P. R. Beatty, and E. Harris.** 2004. Interferon-dependent immunity is essential for resistance to primary dengue virus infection in mice, whereas T- and B-cell-dependent immunity are less critical. J. Virol. **78:**2701–2710.

68. **Shrestha, B., D. Gottlieb, and M. S. Diamond.** 2003. Infection and injury of neurons by West Nile encephalitis virus. J. Virol. **77:**13203–13213.

68a. **Shrestha, B., and M. S. Diamond.** 2004. Role of CD8$^+$ T cells in control of West Nile virus infection. J. Virol. **78:**8312–8321.

69. **Silverman, R. H.** 1997. 2-5A-dependent RNase L: a regulated endoribonuclease in the interferon system, p. 115. *In* E. G. D'Alessio and J. F. Riordan (ed.), Ribonucleases: structures and functions. Academic Press, New York, N.Y.

70. **Stark, G. R., I. M. Kerr, B. R. Williams, R. H. Silverman, and R. D. Schreiber.** 1998. How cells respond to interferons. Annu. Rev. Biochem. **67:**227–264.

71. **Stojdl, D. F., N. Abraham, S. Knowles, R. Marius, A. Brasey, B. D. Lichty, E. G. Brown, N. Sonenberg, and J. C. Bell.** 2000. The murine double-stranded RNA-dependent protein kinase PKR is required for resistance to vesicular stomatitis virus. J. Virol. **74:**9580–9585.

72. **Veeraswamy, R. K., M. Cella, M. Colonna, and E. R. Unanue.** 2003. Dendritic cells process and present antigens across a range of maturation states. J. Immunol. **170:**5367–5372.

73. **Wang, T., T. Town, L. Alexopoulou, J. F. Anderson, E. Fikrig, and R. A. Flavell.** 2004. Toll-like receptor 3 mediates West Nile virus entry into the brain causing lethal encephalitis. Nat. Med. **10:**1366–1373.

73a. **Wang, Y., M. Lobigs, E. Lee, and A. Mullbacher.** 2003. CD8$^+$ T cells mediate recovery and immunopathology in West Nile virus encephalitis. J. Virol. **77:**13323–13334.

74. **Williams, B. R.** 1999. PKR: a sentinel kinase for cellular stress. Oncogene **18:**6112–6120.

75. **Williams, B. R.** 2001. Signal integration via PKR. Sci. STKE *2001:*RE2. [Online.] http://stke.sciencemag.org/.

76. **Xiao, S. Y., H. Guzman, H. Zhang, A. P. Travassos da Rosa, and R. B. Tesh.** 2001. West Nile virus infection in the golden hamster (Mesocricetus auratus): a model for West Nile encephalitis. Emerg. Infect. Dis. **7:**714–721.

77. **Yakub, I., K. M. Lillibridge, A. Moran, O. Y. Gonzalez, J. Belmont, R. A. Gibbs, and D. J. Tweardy.** 2005. Single nucleotide polymorphisms in genes for 2′-5′-oligoadenylate synthetase and RNase L inpatients hospitalized with West Nile virus infection. J. Infect. Dis. **192:**1741–1748.

78. **Yang, Y. L., L. F. Reis, J. Pavlovic, A. Aguzzi, R. Schafer, A. Kumar, B. R. Williams, M. Aguet, and C. Weissmann.** 1995. Deficient signaling in mice devoid of double-stranded RNA-dependent protein kinase. EMBO J. **14:**6095–6106.

79. **Yoneyama, M., M. Kikuchi, T. Natsukawa, N. Shinobu, T. Imaizumi, M. Miyagishi, K. Taira, S. Akira, and T. Fujita.** 2004. The RNA helicase RIG-I has an essential function in double-stranded RNA-induced innate antiviral responses. Nat. Immunol. **5:**730–737.

80. **Zhang, B., J. Tanaka, L. Yang, M. Sakanaka, R. Hata, N. Maeda, and N. Mitsuda.** 2004. Protective effect of vitamin E against focal brain ischemia and neuronal death through induction of target genes of hypoxia-inducible factor-1. Neuroscience **126:**433–440.

81. **Zhou, A., J. Paranjape, T. L. Brown, H. Nie, S. Naik, B. Dong, A. Chang, B. Trapp, R. Fairchild, C. Colmenares, and R. H. Silverman.** 1997. Interferon action and apoptosis are defective in mice devoid of 2′,5′-oligoadenylate-dependent RNase L. EMBO J. **16:**6355–6363.

82. **Zhou, A., J. M. Paranjape, S. D. Der, B. R. Williams, and R. H. Silverman.** 1999. Interferon action in triply deficient mice reveals the existence of alternative antiviral pathways. Virology **258:**435–440.